Chirped pulse enhancement of multiphoton absorption in molecular iodine

Vladislav V. Yakovlev, Christopher J. Bardeen, Jianwe Che, Jianshu Cao, and Kent R. Wilson
Department of Chemistry and Biochemistry, University of California, San Diego, La Jolla, California 93093-0339

(Received 12 September 1997; accepted 4 November 1997)

Chirp effects on three photon absorption yields in I_2 vapor are investigated using femtosecond pulses with center wavelengths in the region 550–600 nm. Enhancements of as much as a factor of 3 are observed for chirped pulses with respect to transform-limited, zero chirp pulses. Theoretical considerations and model calculations suggest that wave packet dynamics play an important role. © *1998 American Institute of Physics.* [S0021-9606(98)01906-0]

I. INTRODUCTION

Multiphoton processes play an important role in many areas of science, including photochemistry,[1] fluorescence imaging,[2] photoionization,[3] and the generation of plasmas and x rays.[4] It is well known that resonant intermediate states can enhance the multiphoton absorption process by orders of magnitude,[5] and this enhancement provides the basis of the resonance enhanced multiphoton ionization (REMPI) detection technique in analytical chemistry. The practical importance of multiphoton absorption, coupled with recent advances in ultrafast laser technology, has lead to a surge of interest in the effects of femtosecond pulses on such processes. For example, it is hoped that by shortening the length of time during which the absorption occurs, one can avoid intramolecular energy redistribution and the subsequent formation of multiple molecular ion fragments.[6,7] The use of ultrashort pulses, with their broad spectra, complicates the analysis of such experiments. Instead of considering only a few molecular eigenstates, it becomes necessary to consider the dynamics of coherent superposition states, or wave packets.

In this paper, we study the effects of the linear chirp of a femtosecond pulse on the multiphoton absorption process in iodine vapor.[8] The phase $\phi(\nu)$ of the electric field can be written as a Taylor expansion in the frequency (ν) domain,

$$\phi(\nu)=\phi(0)+\phi'(0)\,\nu+\tfrac{1}{2}\phi''(0)\,\nu^2+\cdots, \tag{1}$$

where the central frequency of the pulse has been set to 0. If we neglect cubic and higher-order phase terms, the quadratic phase term determines the linear chirp via the relation[9]

$$\tau(\nu)=2\pi\,\frac{\partial\phi(\nu)}{\partial\nu}\propto\phi''(0)\,\nu, \tag{2}$$

where $\tau(\nu)$ is the group velocity delay and $\phi''(0)$ is the linear chirp. For a positively chirped pulse ($\phi''>0$), the low-frequency components arrive first, while a negatively chirped pulse has the opposite ordering. A transform-limited pulse is of the shortest possible duration, with $\phi''=0$. Our data for the three photon absorption (3PA) in I_2 at visible wavelengths demonstrates how the phase structure of the light field couples to the nuclear dynamics of the molecule, resulting in a complex dependence of the 3PA yield on the chirp of the pulse. In particular, at the wavelength of 570 nm, we observe a factor of 3 enhancement in the 3PA yield for a positively chirped pulse relative to the shortest, transform-limited pulse. Preliminary calculations suggest that this enhancement results from a combination of wave packet motion and the position-dependent energy detuning of the electronic states and is different in origin from that observed in Na_2.[10]

II. EXPERIMENT

In these experiments we use tunable femtosecond pulses with center wavelengths ranging from 550 to 600 nm, the second harmonic of the output of an optical parametric amplifier seeded by a white light continuum.[11] A prism compressor is used to compress the pulses and the linear chirp is varied by inserting more or less prism material (BK-7) in the beam. Frequency resolved polarization optical gating[12] and second harmonic autocorrelation are used to characterize the amplitude and the phase of the pulses. Both methods are in reasonably good agreement with each other and with estimations of the linear chirp of the pulse obtained from dispersion calculations. The shortest pulse widths, which we refer to as transform limited, are 30–40 fs for all wavelengths. The maximum energy of the pump pulses is typically about 0.5 μJ and is attenuated using thin gelatin neutral density filters that do not affect the pulse chirp. The focal spot is approximately 50 μm in diameter. The molecular iodine is contained in a quartz bulb that is heated to 40 °C, resulting in a vapor pressure of approximately 1 Torr. The laser-induced fluorescence (LIF) signal at 340 nm, resulting from collisionally relaxed $D'\rightarrow A'$ emission,[13] is detected. The dependence of the LIF signal on pulse energy varies as the cube of the energy at lower energies before saturating slightly near the maximum pulse energy. By changing the sample temperature, the optical density was varied without any observable effect on the signal's chirp dependence.

III. RESULTS

Figure 1 shows the measured LIF signal as a function of pulse chirp for pulses centered as 550, 570, and 600 nm. All

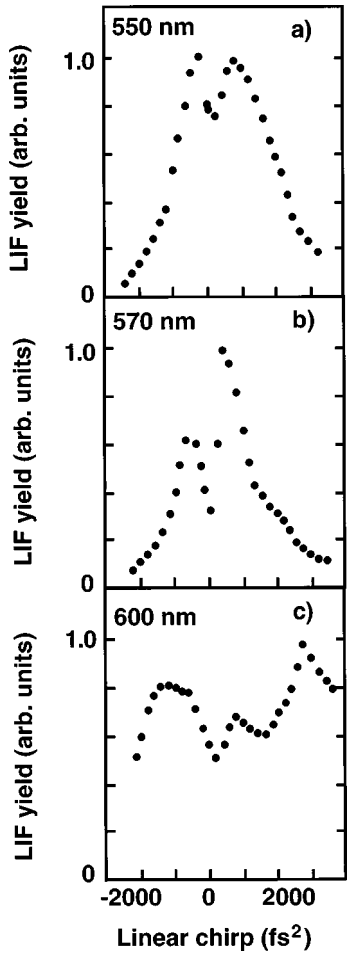

FIG. 1. (a) Experimentally measured laser-induced fluorescence yield resulting from three photon absorption at 550 nm in I_2 vapor as a function of linear chirp, $\phi''(0)$. (b) As in (a), but for a laser pulse centered at 570 nm. (c) As in (a), but for a laser pulse centered at 600 nm. All curves have been normalized to unity.

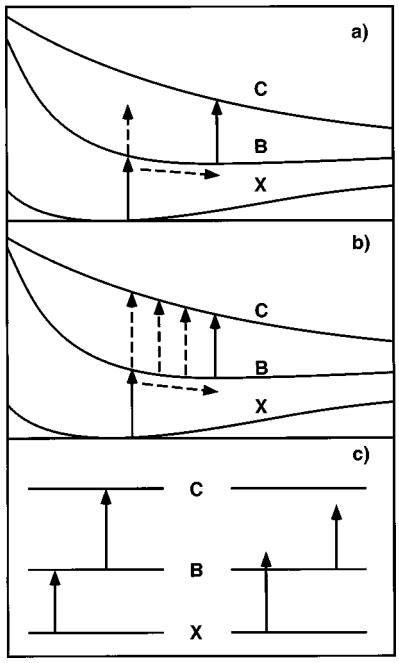

FIG. 2. Schematic representation of three mechanisms for chirped pulse enhancement of multiphoton absorption. Only the first two stages ($X \rightarrow B \rightarrow C$) of the three photon absorption in I_2 are shown. (a) The *time-delay resonance* mechanism, in this case positive chirp leads to the high-frequency components of the pulse catching the moving wave packet in resonance with the $B \rightarrow C$ transition. (b) The *wave packet following* mechanism, where the change in instantaneous pulse frequency follows the change in the wave packet's electronic transition energy. (c) The *sequential resonance* mechanism, where the chirp leads to an ordering of frequencies that is resonant first with the $X \rightarrow B$ transition and then with the $B \rightarrow C$ transition, sequentially transferring population.

the data curves were taken with pulse energies of about 100 nJ, which is within the weak response (cubic dependence of signal on pulse energy) regime. At higher pulse energies, the chirp dependences of the LIF broaden slightly but retain the same general shapes. At none of the three pulse wavelengths do we observe a simple dependence of the 3 PA yield on chirp. If the 3 PA were completely nonresonant we would expect the 3 PA yield to be maximized for the transform-limited pulse, with the highest peak intensity, and to fall off quickly as the chirp increases and the peak intensity decreases. On the other hand, if the 3 PA were due to a completely resonant sequential process, neglecting wave packet motion, its yield would be independent of chirp, since the population can wait a relatively long time on each intermediate state before absorbing another photon. Both of these limiting cases predict a LIF signal that varies as the cube of the pulse energy and depends symmetrically on pulse chirp. As Fig. 1 shows, the observed dependence of the LIF yield on chirp is complex and asymmetric at all wavelengths used. Most striking is the three-fold enhancement at 570 nm obtained for a positively chirped pulse. The phase term $\phi'' = 400\ \text{fs}^2$ corresponds to an increase in pulse duration from 30 to 45 fs. At both 550 and 570 nm, the LIF signal is seen to decrease quickly as the pulse becomes longer than 100 fs, but at 600 nm there is no systematic decay over this range of the LIF relative to the transform limit value as the chirp is increased. At 600 nm, a pulse that is five times longer than transform limit ($\phi'' = +/-2000\ \text{fs}^2$) results in roughly the same LIF signal.

IV. DISCUSSION AND NUMERICAL RESULTS

Some insight can be gained by considering the process in the time domain, where the multiply excited vibronic states give rise to nonstationary wave packets propagating on the appropriate electronic potential energy surfaces (PES's). The pulses used in these experiments are resonant with the first $X-B$ transition in I_2, and from our previous work[14] we know that wave packets are created on the B state. As the initially created wavepacket changes position, the probability of absorbing additional photons also changes due to several factors, including the position dependence of the energy difference between the PES's and the transition dipole moment. If the frequency of the excitation pulse is changing in time as well, as is the case for a chirped pulse, we can expect some coupling between the light filed dynamics and those of the molecule. In Fig. 2, we outline three effects that give rise to a chirp dependence in the quasiresonant multiphoton absorption process that occurs in I_2. The first two, *time-delay resonance* and *wave packet following*, are due to the nonstationarity of the intermediate populations in the multiphoton

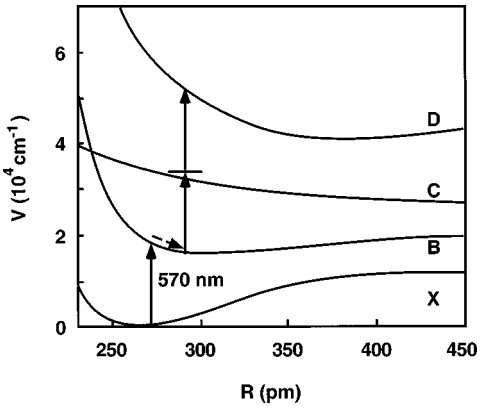

FIG. 3. Iodine potential energy surfaces used in the calculations of resonantly enhanced three photon absorption.

process, while the third, *sequential resonance*, is solely the result of the level structure of the molecule and does not rely on wave packet dynamics. While these effects can be distinguished in principle, in practice they may not be easily separable, and for I_2 all three most likely play some role.

When an ultrashort pulse is used to drive a multiphoton process, all the transitions must occur within the pulse duration. If the pulse is transform limited, the time window in which these transitions can occur is minimized. Since there is little time for the intermediate populations to evolve, the efficiency of the process will be determined by the Franck–Condon factors of the relevant states near the original ground state position. This situation is different for a chirped pulse, where the relative arrival times of the respective frequency components can be adjusted. For instance, consider the situation of I_2 when the low-frequency leading edge of a positively chirped pulse creates some population on the *B* state, which propagates until it reaches a region of the PES, where it can be resonantly excited to the *C* state by the trailing high-frequency edge of the pulse. If the chirp is adjusted correctly, the high-frequency components arrive when their energy matches the PES difference at the location of the moving wave packet, resonantly enhancing the second absorption. By using a chirped pulse to delay the arrival time of one frequency component with respect to another, we can use the wave packet motion to bring the intermediate population on the *B* state into resonance with the *C* state, resulting in an enhancement of the absorption. We term this effect *time-delay resonance*, and it is shown schematically in Fig. 2(a). A negatively chirped pulse can give rise to the same effect, although it may not be the same as for a positively chirped pulse. A ''red–blue'' sequence of photon interactions starts and ends at different points on the PES than does a ''blue–red'' sequence, and there is no reason to expect that both will result in the same enhancement of the 3PA. In fact, the pronounced asymmetry in the chirp dependences in Fig. 1 shows the nonequivalence of positive and negative chirps and proves that the observed effects cannot be due simply to lengthening the pulse in time.

A second dynamical mechanism that can lead to an enhancement of the 3PA is the *wave packet following* effect shown in Fig. 2(b). As the wave packet moves, the transition energy becomes time dependent, and a chirp that follows this dependence, while not necessarily exactly on resonance, will be more effective in transferring population to the higher state.[15,16] Rather than timing the arrivals of two color components of the pulse to fulfill a resonance condition, as in the *time-delay resonance* case, *wave packet following* relies on matching the rate of change of the light frequency with that of the electronic transition. The key quantity is the velocity of the wave packet and not its position at two points in time. The velocity of the wave packet starting in the Franck–Condon region is fixed, so this effect is expected to occur only for one sign of the chirp, usually negative, since the separation between states in the Franck–Condon region usually decreases as a function of internuclear distance (see Figs. 2 and 3).

A third mechanism that does not involve dynamics at all (i.e., it occurs even when the wave packets are ''frozen'') is the *sequential resonance* effect[17] outlined in Fig. 2(c). Sup-

TABLE I. Electronic states.

Parameters[a]	*X*	*B*	*C*	*D*
$V(r)$	$T_e+D_e(1-e^{-\beta(r-r_e)^2})$	$T_e+D_e(1-e^{-\beta(r-r_e)^2})$	$T_e+Ae^{-\beta(r-r_e)}$	$T_e+D_e+be^{-\beta r^p}+\frac{C_{12}}{r^{12}}-\frac{C_1}{r}-\frac{C_3}{r^3}-\frac{C_4}{r^4}-\frac{C_6}{r^6}$
T_e	0	15 769	27 257	41 024
D_e	12550	4381	⋯	31 155
β	1.871	1.876	1.512	0.214
r_e	2.663	3.016	1.852	⋯
A	⋯	⋯	24 585	⋯
b	⋯	⋯	⋯	258 913
p	⋯	⋯	⋯	2.16
C_1	⋯	⋯	⋯	116 141
C_3	⋯	⋯	⋯	44 000
C_4	⋯	⋯	⋯	580 000
C_6	⋯	⋯	⋯	1 000 000
C_{12}	⋯	⋯	⋯	840 000 000

[a]Units are cm^{-1} for energy and angstroms for coordinates.

pose the first transition $(X-B)$ is resonant with the low-frequency part of the pulse and the second $(B-C)$ is resonant at a higher frequency. In this case, a positively chirped pulse can sequentially transfer population from X to B to C much more effectively than a negatively chirped pulse. As in the case of *wave packet following*, this effect only occurs for one sign of the chirp, since the electronic level spacings are uniquely determined.

In order to gain insight into the processes leading to the observed chirp effects, we have performed some preliminary calculations. The 3PA process can involve a large number of rovibronic states. A full calculation of the process, taking into account all possible states, is a daunting task even for a simple diatomic like I_2. As a first approximation, we utilize the four electronic state model shown in Fig. 3. The resulting Hamiltonian can be written as

$$H=\frac{\hat{p}^2}{2m}+\begin{bmatrix} V_X(r) & -\mu_{BX}E^*(t) & 0 & 0 \\ -\mu_{BX}E(t) & V_B(r) & -\mu_{CB}E^*(t) & 0 \\ 0 & -\mu_{CB}E(t) & V_C(r) & -\mu_{DC}E^*(t) \\ 0 & 0 & -\mu_{DC}E(t) & V_D(r) \end{bmatrix}.$$

The analytical forms and parameters of the PES's used in these calculations are listed in Table I. While the ground (X) and first excited (B) states are very well characterized spectroscopically, there is considerably less information on the high-lying ion pair states (D).[18,19] Even less is known about the intermediate covalent states (C).[20] Thus there is considerable uncertainty in our example model, in particular, in the form of the D state, and the potential we use differs significantly from the form of the $D(^1\Sigma_u^+)$ state derived from absorption and emission experiments.[21] The numerical algorithm used to calculate the dynamics is the split-operator method using a fast Fourier transform.[22] The light fields were those measured experimentally, and the system had a vibrational thermal distribution corresponding to the experimental conditions but no rotational distribution $(J=0)$. The LIF signal was assumed to be directly proportional to the population of the final D state.

A comparison of theory and experiment at 570 nm is shown in Fig. 4. The qualitative agreement is quite good at this wavelength, as it also is at 550 nm. The calculation predicts a much stronger chirp enhancement at 600 nm than is actually observed, and this may be due to the involvement of multiple electronic states that are resonant at that pump wavelength and are not taken into account. The calculated dependence is quite sensitive to the details of the PES, and using literature values for the D state results in a completely different chirp dependence. Removing the kinetic energy term from our model Hamiltonian (and thus freezing the wave packet motion) results in a calculated LIF signal peaked at the transform-limited pulse, implying that without wave packet motion the 3PA is largely nonresonant and the stationary *sequential resonance* mechanism does not play a role. This contrasts with the experiments by Assion *et al.*,[10] where the enhancement of photoionization yield was determined to be primarily due to this effect. In those experiments, the excitation pulse was tuned to the high-energy side of the ground state absorption spectrum, so that a positively chirped pulse was the most effective in transferring population to the first excited state, where it then absorbed more photons. Like the *sequential resonance* effect, *wave packet following* should only maximize the signal for one sign of the chirp and is inconsistent with the observed enhancement with both positive and negative chirp. We conclude that the *time-delay resonance* effect, where the molecule absorbs a first photon and then undergoes nuclear motion to bring its excited state absorption into resonance with subsequent photons, must play an important role in the observed enhancement. We emphasize that these preliminary calculations do not preclude all three of the above-mentioned effects from playing some role in the 3PA of I_2 at these wavelengths.

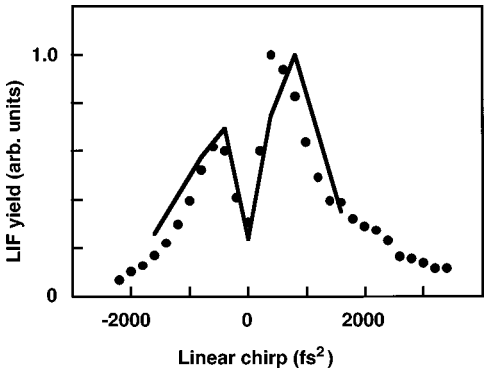

FIG. 4. Comparison of the experimentally measured three photon LIF signal (points) and the signal calculated using the four PES's whose parameters are listed in Table I. The experimentally measured electric fields were used in the calculation.

In summary, we have demonstrated the importance of the phase structure of a femtosecond pulse in affecting the yield of a multiphoton process. A process that proceeds through several resonant or quasiresonant intermediate states on which nuclear motion can occur can be expected to be sensitive to pulse chirp, and our observation of a factor of 3 enhancement shows the possible benefits of using a non-transform-limited pulse. A more extended theoretical analysis of intrapulse dynamical effects in multiphoton processes is given elsewhere.[16] The coupling of the molecule's coherent nuclear dynamics with the phase coherence of the ultrashort pulse provides a means of coherent control over multiphoton processes.

[1] M. Blackwell, P. Ludowise, and Y. Chen, J. Chem. Phys. **107**, 283 (1997).
[2] W. Denk, J. H. Strickler, and W. W. Webb, Science **248**, 73 (1990).
[3] E. Constant, H. Stapelfeldt, and P. B. Corkum, Phys. Rev. Lett. **76**, 4140 (1996).
[4] M. M. Murnane, H. C. Kapteyn, M. D. Rosen, and R. W. Falcone, Science **251**, 531 (1991).
[5] Y. R. Shen, *The Principles of Nonlinear Optics* (Wiley, New York, 1984).
[6] J. J. Yang, D. A. Gobeli, and M. A. El-Sayed, J. Phys. Chem. **89**, 3426 (1989).
[7] R. Weinkauf, P. Aicher, G. Wesley, J. Grotemeyer, and E. W. Schlag, J. Phys. Chem. **98**, 8381 (1994).
[8] K. Chen, L. E. Steenhoek, and E. S. Yeung, Chem. Phys. Lett. **59**, 222 (1978).
[9] E. B. Treacy, IEEE J. Quantum Electron. **5**, 454 (1969).
[10] A. Assion, T. Baumert, J. Helbing, V. Seyfried, and G. Gerber, Chem. Phys. Lett. **259**, 494 (1996).
[11] K. R. Wilson and V. V. Yakovlev, J. Opt. Soc. Am. B **14**, 444 (1997).
[12] R. Trebino and D. J. Kane, J. Opt. Soc. Am. A **10**, 1101 (1993).
[13] J. Tellinghuisen and L. F. Phillips, J. Phys. Chem. **90**, 5108 (1986).
[14] C. J. Bardeen, J. Che, K. R. Wilson, V. V. Yakovlev, V. A. Apkarian, C. C. Martens, R. Zadoyan, B. Kohler, and M. Messina, J. Chem. Phys. **106**, 8486 (1997).
[15] M. Sterling, R. Zadoyan, and V. A. Apkarian, J. Chem. Phys. **104**, 6497 (1996).
[16] J. Cao and K. R. Wilson, J. Chem. Phys. **106**, 5062 (1997).
[17] J. Cao, J. Che, and K. R. Wilson, J. Phys. Chem. (submitted).
[18] J. C. D. Brand and A. R. Hoy, Appl. Spectrosc. Rev. **23**, 285 (1987).
[19] R. S. Mulliken, J. Chem. Phys. **55**, 288 (1971).
[20] C. Teichteil and M. Pelissier, Chem. Phys. **180**, 1 (1994).
[21] J. Tellinghuisen, Can. J. Phys. **62**, 1933 (1984).
[22] R. Kosloff, Annu. Rev. Phys. Chem. **45**, 145 (1994).